Indian Journal of Chemical Technology
Vol. 30, May, 2023 pp. 331-341
DOI: 10.56042/ijct.v30i3.70061

Mentha piperita extract as a natural product for the corrosion inhibition of low carbon steel in a polluted NaCl environment: Chemical, electrochemical and biological studies

Abd El-Aziz S Fouda*[,1], Ameena M Al-Bonayan[2], Ali M Elazly[3] & Mohamed F Attia[4]

[1,*]Faculty of Science, Mansoura University, Mansoura-35516, Egypt,

[2]Faculty of Science, Umm Al-Qura University, Makkah, KSA

[3]Nile Higher Institute for Engineering and Technology, EI-Mansoura, Egypt

[4]Faculty of Technological Industry and Energy, Delta Technological University, Qewasnia, EI-Menoufia, Egypt

E-mail: asfouda@mans.edu.eg

Received 3 January 2023; accepted 17 March 2023

The impact of aqueous Mentha piperita extract (MPE) as a corrosion inhibitor for low carbon steel (LCS) in NaCl/Na_2S solution has been investigated using chemical and electrochemical techniques to evaluate the protection performance of MPE. "As the concentration of the extract increased, the protection efficiency (PE) increased, reaching 91.2% at 300 ppm, whereas the increase in temperature favoured to slow decrease".The extract has been physically adsorbed on the metal surface according to the Temkin isotherm. Polarization data reveal that this extract acts as a mixed inhibitor. The mechanism of corrosion protection of MPE has been discussed from electrochemical techniques. MPE has been adsorbed on LCS obeying Temkin isotherm. Surface morphology techniques such as scanning electron microscopy (SEM) and atomic force microscopy have been used to demonstrate the creation of a protective coating on the LCS in the presence of MPE. The extract inhibits the bacterial activity of *Escherichia coli*.

Keywords: Corrosion inhibition, Low carbon steel, NaCl/Na_2S, Mentha piperita extract (MPE), Temkin isotherm

Low carbon steel (LCS) appears to be widely employed for structural purposes because of its low cost. However, its susceptibility to rusting in humid air and rapid dissolution rate in acidic solutions are significant drawbacks for its application on a broader scale without protection. Corrosion is a naturally occurring phenomenon that deteriorates a material or its properties because of a reaction with its environment. Corrosion can cause dangerous and expensive damage to everything from pipelines, bridges and public buildings to vehicles, water, and wastewater systems, and even home appliances. It is one of the most serious problems in the oil and gas industry. In general, hydrochloric acid is employed in industries for cleaning, descaling, and pickling steel structures such as reactors, agitators, pumps, drains, and so on, which are prone to significant metal dissolution. The use of inhibitors is the most feasible corrosion prevention approach for slowing down the aggressiveness of this acid. The use of organic extracts is one of the most widely practical methods for protection of metals and alloys against corrosion, since adding extracts does not cause disruption of the industrial process. In previous years, numerous extracts have been extracted or selected from existing plants, and it has been found that the finest extracts are those having a center for π electron donation (usually heightened by the presence of heteroatoms in aromatic compounds), while others may be obtained from extracts of obviously occurring compounds[1-3]. Extracts derived from plants are significant because they are environmentally friendly[4,5], nontoxic and don't contain heavy metals. It has been established that sulfur and/or nitrogencontaining heterocyclic compounds with various substituents are effective corrosion extracts in different solutions over a wide *p*H range. The PE of an organic compound mainly depends on its ability to adsorb on the metal surface. The protective nature of the adsorbed compact barrier film is influenced by the nature of the metal surface and electronic structure of inhibiting molecules. The adsorption of nitrogenous compounds is ascribed to the effects of the functional groups connected with aromatic rings parallel to the metal surface[6]. Indeed,

various investigations on corrosion inhibition utilizing plant extract[7-9], pure chemicals[10,11] and essential oils[12–21] have been performed in the last decade. They have all been identified as excellent inhibitors for various metals and alloys in various acidic settings. The current study aims to evaluate the protection efficiency (PE) of the investigated MPE in directing the corrosion of LCS in polluted NaCland to analyze the protective film formed on the LCS surface using scanning electron microscopy (ESM), energy dispersive X-ray (EDX) and AFM techniques. Finally,the extract's bacterial activity against Escherichia coli was investigated.

Experimental Section

Materials and solutions

The material used is LCS, which has the following chemical conformation (weight %): 0.014 C, 0.004 Si, 0.36 Mn, 0.25 P and the rest is iron.

Preparation of the extract

The origins of Mentha Piperita are assumed to be in Northern Africa and the Mediterranean. Mint is cited as a stomach pain reliever in the Ebbers Papyrus, an ancient Egyptian medical document dating from 1550 BC. In Egypt, the mint was so valuable that it was utilized as a type of currency.

An aqueous extract of MP was prepared by powdering a reasonable number of plant leaves to get 500 g of powdered materials. These quantities were soxholated with double distilled water, dried until frozen, weighed, and stored at 4^{o}C until needed. The 3.5 percent NaCl and 16 ppm Na_2S solutions were created by liquefying the appropriate quantity of salts in double distilled water. All the compounds were of the AR grade. The studies were performed in settings that were naturally non bubbling and stagnant. The addition of extract had no effect on the *p*H of the medium.

Preparation of bacterial agriculture media

Dissolve 50 g of the medium in L of double distilled water by heating. Sterilize for 15 minutes in an autoclave at 121^{o}C. Cool to 45-50^{o}C and then thoroughly combine and distribute into plates. Allow the plates to harden. The temperature of the prepared medium should be between 8 and 15 degrees Celsius. Violet red is the colour. The results of chemical tests in the literature with aqueous extract of MPE contain phytochemicals such as diterpenes, steroids, tannin, flavonoids, carbohydrates, alkaloids, phenols, coumarin, and saponins, whereas the ethanolic extract also contains the same chemicals except tannin, cardiac glycosides, and saponin[22,23].

Methods

The weight loss (WL) approach is well known as the most extensively used methodology for assessing inhibition effectiveness. The procedure for WL determination was similar to that reported earlier[24]. Seven samples of LCS (2 × 2 × 0.1 cm as a dimension) were reweighed using a digital balance (Model Denver Instrument) and dipped in 100 ml of corroding medium (in open beakers) with and without different concentrations (50-300 ppm) of the extract at temperatures from 25-40°C for a total period of 180 min dipped period. The samples were withdrawn from the solution at intervals of 30 min immersion, rinsed with water, scrubbed with a bristle brush under running water, dried and reweighed". Triplicate experiments were set up for each concentration of extract for reliability.

Cathodic and anodic polarization curves were recorded in the potential region OCP ± 250 mV (SCE) as a function of concentration at a sweep rate of 0.2 mV/s. A cell with three electrodes was used. LCS as the working electrode, reference electrode was saturated calomel electrode (SCE) and counter electrode was Pt foil. From PP curves, corrosion data such as E_{corr}, corrosion current $i_{corr,}$ anodic Tafel slopes, β_a and cathodic slopes β_c were computed.

EIS spectra were recorded in the frequency ranges 10^5 Hz and 0.1 Hz with amplitude of 10 mV peak to peak at the open-circuit potential. The values of charge transfer resistance (R_{ct}) and double layer capacitance (C_{dl}) were calculated.

The EFM was carried out at two different frequencies: 2 and 5 Hz. Because the base frequency was 0.1 Hz, the waveform was repeated every 1s, which was required for good resolution of the current response. The largest peaks were utilized to calculate the corrosion current density (i_{corr}), Tafel lines (β_c and β_a), and fitting together factors CF-2 and CF-3[25].

All electrochemical tests were carried out using a Gamry PCI300/4 Potentiostat/Galvanostat/Zra-analyzer. For data fitting and calculation, a personal computer running DC 105 software for PP, EIS300 program for EIS, EFM140 software for EFM, and Echem Analyst 5.21 was utilized.

Surface examination study

The coin surfaces were examined using a JSM-6390AL model before and after dipping in corrosive conditions for one day. Meanwhile, the components in

the material were analyzed using an energy dispersive spectrometer (EDX). The nature of the film generated on the surface of the metal coins was investigated using these techniques. The roughness of the surfaces was checked utilizing atomic force microscopy (AFM) at the Faculty of Engineering, Mansoura University, Egypt.

Results and Discussion

WL measurements

Figure 1 contains theWL-time plots of LCS in Polluted NaCl solution with existing and nonexistent altered concentrations of MPE. The corrosion rate (mg cm^{-2} min^{-1}), degree of surface coverage (Θ) and PE% at 25°C are tabulated in Table 1. Inspection of Table 1 reveals that the corrosion rate of LCS is highly reduced upon the addition of MPE due to the large coverage of the LCS surface by extracted molecules. This result indicates that MPE acts as a good corrosion inhibitor for LCS in this aggressive medium.(θ) and %PE are calculated using Eq. (1)[26]

$$\% PE = \frac{Wo - Wi}{Wo} \times 100 = \theta\, x100 \quad \ldots(1)$$

Where, W_o and W_i are the mass losses in the absence and presence of extract, respectively. As revealed from the data in Table 1, the extract has quite a high %PE that reaches 91.2% for 300 ppm of the extract. By increasing the extract concentration, the percent PE increased. The extract can be adsorbed on the LCS surface due to unpaired electrons present on their oxygen atoms and/or electrostatic attraction, according to the chemical structures of the extract. The extract's adsorption on the metal provides a charge and mass transfer barrier, which reduces the metal's contact with the corrosive environment. As a result, the metal's corrosion rate is lowered.

Impact of temperature

The WL technique was used to investigate the impact of temperature on the corrosion characteristics of LCS in polluted NaCl solution with and without altered doses of MPE in the temperature range of 25- 40°C. Temperature has a significant impact on the PE of the extract on the LCS, as shown in Table 2 and Fig. 2 (a-c), which decreases as temperature rises.

Arrhenius processes are commonly used to describe corrosion reactions, and the rate (k_{corr}) can be stated using the equation in Eq. (2):

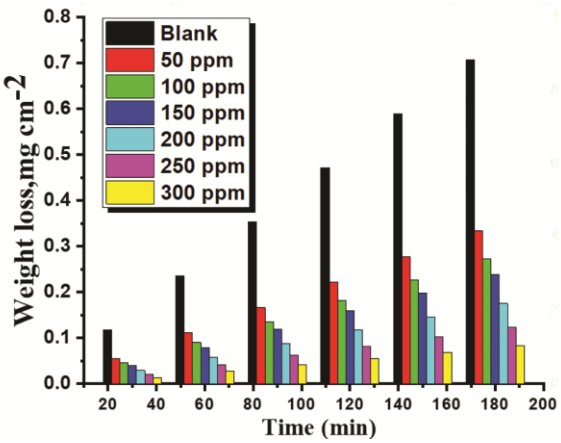

Fig. 1 — WL- time diagram for the dissolution of LCS in polluted NaCl with and without altered concentrations of MPE at 25°C

Table 1 — Impact of MPE concentrations on the WL (mg cm^{-2}) and (Θ) of LCS in 3.5 percent NaCl + 16 ppm Na_2S 25°C

Conc. ppm	25°C		
	WL, mg cm^{-2}	Θ	% PE
Blank	0.70710±0.1721	----	---
50	0.3333±0. 2303	0.519	51.9
100	0.2711±0. 2644	0.617	61.7
150	0.2381±0. 2885	0.663	66.3
200	0.1557±0. 2028	0.780	78.0
250	0.1027±0. 2336	0.855	85.5
300	0.0620±0. 2818	0.912	91.2

Table 2 — Effects of MPE concentrations on LCS WL and protection efficiency (percent PE) in 3.5 percent NaCl + 16 ppm Na_2S (polluted NaCl) at various temperatures

Conc. ppm	30°C		35°C		40°C	
	WL mg cm^{-2}	% PE	WL mg cm^{-2}	% PE	WL, mg cm^{-2}	% PE
Blank	0.73230±0.2309	---	0.7702±0. 3302	---	0.83333±0. 2635	---
50	0.3629±0. 2027	50.4	0.4062±0.2309	47.3	0.4642±0. 2025	44.3
100	0.2990±0. 2333	59.2	0.3397±0.1732	5598	0.3977±0.1734	52.3
150	0.2598±0. 1763	64.5	0.3101±. 2309	59.7	0.3679±0. 2811	55.9
200	0.1866±0. 1452	74.5	0.2279±0.0176	70.4	0.3009±0. 2810	63.9
250	0.1239±0. 2886	83.1	0.1650±0.0176	78.6	0.2169±0. 2882	74.0
300	0.0889±0. 2027	87.9	0.1086±0. 2335	85.9	0.1778±0.1724	78.7

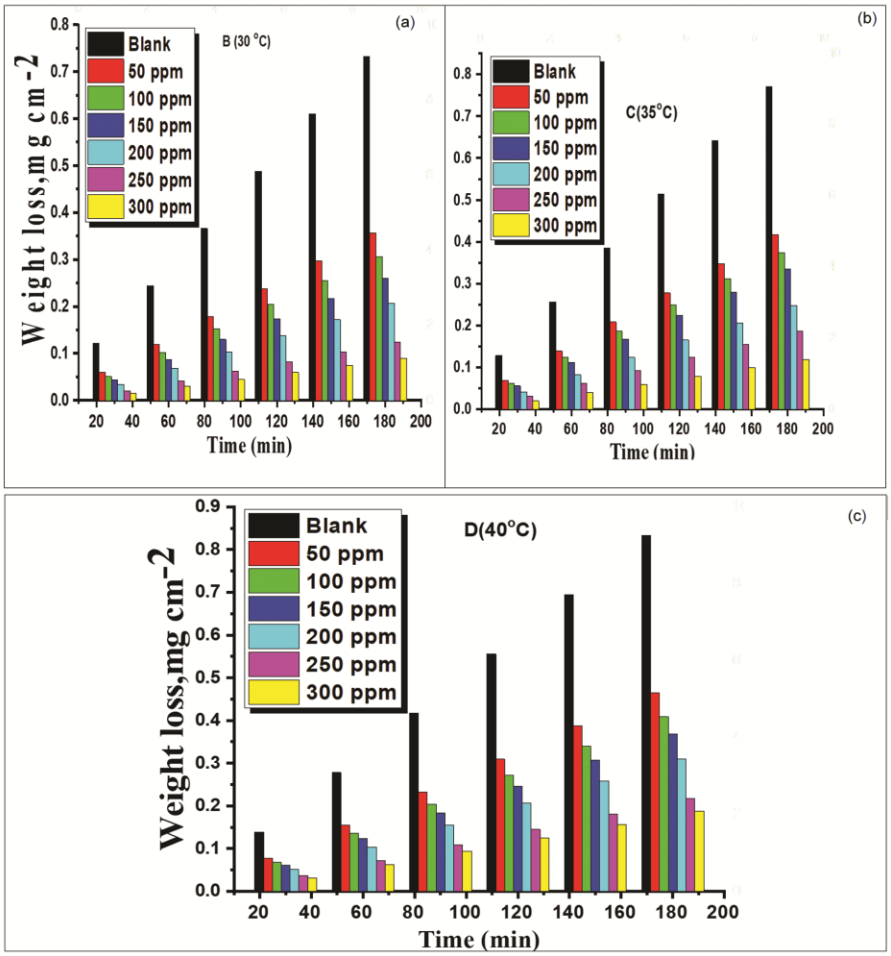

Fig. 2 — (a-c) WL-time diagrams for the corrosion of LCS NaCl/H_2S with and without MPE at altered temperatures

$$"k_{corr} = A\, e^{(-E^*a/RT)"} \quad \ldots(2)$$

Where k_{corr} is the corrosion rate, E^*_a is the apparent activation energy, R is the universal gas constant, T is the absolute temperature, and A is the frequency factor. Fig. 3 shows an Arrhenius plot (log k_{corr} against the reciprocal of temperature (1/T)) followed by straight lines with high correlation coefficients. For the blank and extract, the activation energy E_a^* ranged from 8.5 to 42.7 (Table 3). Physical adsorption or weak chemical interaction between the extract molecules and the LCS surface is indicated by a rise in E_a^* when the extract is present[27]. Eq. (3) is used to compute the activation enthalpy(ΔH^*) and entropy (ΔS^*) utilizing transition state theory:

The Arrhenius equation can also be written as:

$$k_{corr} = RT/Nh_{exp}\, (\Delta S^*/R)\, _{exp}\, (-\Delta H^*/RT) \quad \ldots (3)$$

where h is Planck's constant and N is Avogadro's number. A plot of log k_{corr}/T as a function of 1/T for LCS is shown in Fig. 3(b). Straight lines with a slope of $\Delta H^*/R$ and an intercept of ln R/Nh + $\Delta S^*/R$ were drawn, from which the values of ΔH^* and ΔS^* for the blank and extract were computed. The activation enthalpy, ΔH^*, was 6.0 and 40.8 kJ mol^{-1} for the blank and the extract, respectively, while the activation entropy, ΔS^*, was 177.9 and 271.0 J $mol^{-1}K^{-1}$ for the blank and extract (Table 3). In the absence and presence of extract, the ΔS^* is substantial and negative. This implies that the activated complex in the rate determining step represents an association rather than a dissociation step, meaning that a decrease in disordering takes place on going from reactants to the activated complex[28,29]. The positive sign of ΔH^* indicates that the corrosion process is endothermic

Adsorption isotherms

To study the adsorption behavior of MPE on the LCS surface in the given medium, the adsorption isotherm must be defined to explain the mechanism of

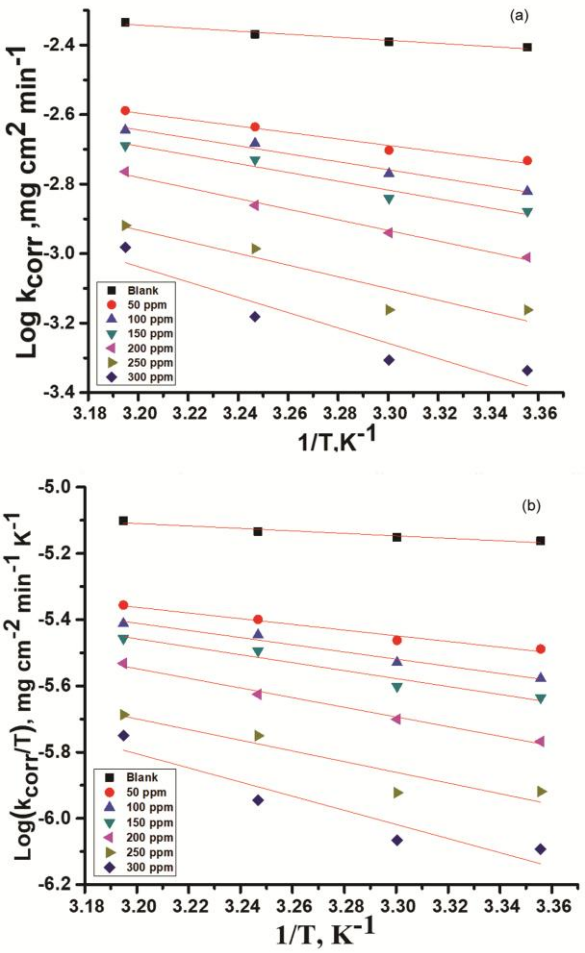

Fig. 3 — (a) Arrhenius plots for the corrosion rate of LCS in NaCl/H_2S in the absence and presence of MPE at different temperatures and (b) Log (k_{corr}/T) versus 1/T for LCS in sulfide-polluted saltwater in the absence and presence of MPE at different temperatures

Table 3 — Activation parameters for LCS corrosion in the absence and presence of various concentrations of investigated MPE

Conc., ppm	E^*_a, kJ mol^{-1}	ΔH^*, kJ mol^{-1}	$-\Delta S^*$, J mol. K^{-1}
Blank	8.5±0.2731	6.0±01452	271.0±0.233
50	18.0±0.3734	16.4±01732	247.5±0.234
100	22.2±0.1742	20.7±02024	234.7±0.145
150	24.5±0.2333	23.0±02021	228.5±0.2027
200	29.5±0.2603	28.0±02022	214.4±0.3179
250	32.6±02309	30.8±01732	207.7±0.3179
300	42.7±01201	40.8±02027	177.9±0.3179

the extract reaction. The best fit isotherm is Temkin adsorption isotherm. On its active sites, the extract is adsorbed on the metal surface. Θ values for altered extract doses at various temperatures were tested by fitting to various isotherms. Therefore, the relation between the dose of the extract (C), (Θ) and the

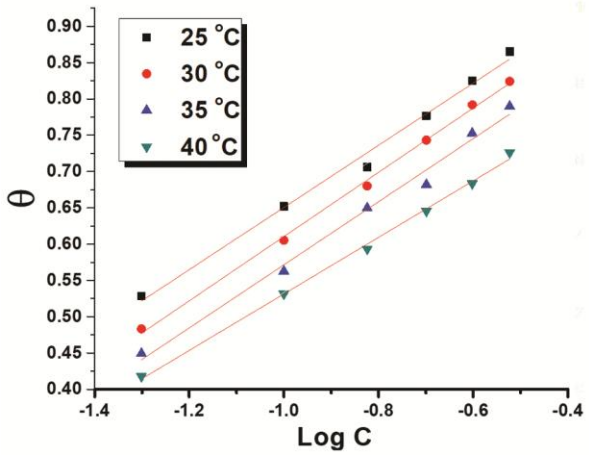

Fig. 4 — Temkin adsorption isotherms for MPE at different temperatures for the LCS in NaCl/H_2S solution

Table 4 — Adsorption parameters for LCS in theabsence and presence of various concentrations of MPE

Temp. K	-Log K_{ads}	$-\Delta G^o_{ads}$ kJ mol^{-1}	$-\Delta H^o$ kJ mol^{-1}	$-\Delta S^o$ J mol^{-1}K^{-1}
298	2.4088	23.9±0.2332	32.5	189.5±0.3756
303	2.2970	23.7±0.5532		185.6±0.4435
308	2.1331	23.1±0.2265		180.7± 0.4967
313	2.2425	24.2±0.4123		181.1± 0.3232

adsorption equilibrium constant (K_{ads}) was obtained from the Temkin adsorption isotherm:

$$a\Theta = \ln K_{ads} C \quad \ldots(4)$$

where (a) is the heterogeneity factor, C is the concentration of extract and K_{ads} is the constant of adsorption equilibrium, which is related to the standard free energy of adsorption (ΔG^o_{ads}) by the equation:

$$\text{“}K_{ads} = (1/55.5) \exp. (\Delta G^o_{ads}/RT)\text{”} \quad \ldots(5)$$

where 55.5 is the concentration of water in mol./L at metal solution interface. The plot of (Θ) as a function of logarithm of the extract dose is shown in Fig. 4. From the plot, straight lines were obtained for the extract, indicating that the experimental data fit well into the Temkin adsorption isotherm. The Temkin isotherm characterizes the chemisorption of uncharged molecules on heterogeneous surfaces. The regression coefficients (R^2) are about 0.99. The departure of the slopes from unity is due to molecular interaction between the adsorbed extract species, which is not considered during the deviation: $\Delta G°_{ads}$ is consistent across all sites and is unaffected by the degree of surface coverage. The data in Table 4 show

that the adsorbate does not interact with one another, i.e., the adsorbate on $\Delta G°_{ads}$ has no effective interaction. Table 4 shows that as the temperature rises, the K_{ads} value drops, indicating that the extract adsorption on the metal surface is reduced. In general, K_{ads} refers to the strength of the bond between the adsorbent and the adsorbate. The ΔG^{o}_{ads} values were derived from this plot, and were negative, indicating that the extract molecules were stable and spontaneously adsorbed on the LCS surface. The heat of adsorption (ΔH^{o}_{ads}) can be determined using Vant Hoff's formula:

$$\text{“Log } K_{ads} = (-\Delta H^{o}_{ads}/2.303\ RT) + \text{constant”} \quad \ldots(6)$$

To calculate the heat of adsorption (ΔH^{o}_{ads}), log $K_{ads}$was plotted against 1000/T (Fig. 5). A straight line was obtained. The absolute values of (ΔH^{o}_{ads}) obtained in this study were lower than 100 kJ mol^{-1}, which is indicative of physisorption, and supports the above mechanism of adsorption. The negative value of ΔH^{o}_{ads} (−32.520 kJ mol^{-1}) in the presence of the extract reflects the exothermic nature of the LCS dissolution process. The activation enthalpies vary in the same manner as the activation energies, supporting the proposed protection mechanism. According to the basic Eq.:

$$\text{“}\Delta G^{o}_{ads} = \Delta H^{o}_{ads} - T\Delta S^{o}_{ads}\text{“} \quad \ldots(7)$$

The adsorption entropy, ΔS^{o}_{ads}, was determined. The large negative entropy values in the presence of this investigated extract indicates that the activated complex in the rate-determining step represents an association rather than dissociation step, implying that disordering decreases as one moves from reactants to the activated complex, and the activated molecules are in a higher order state than at the start [30,31].

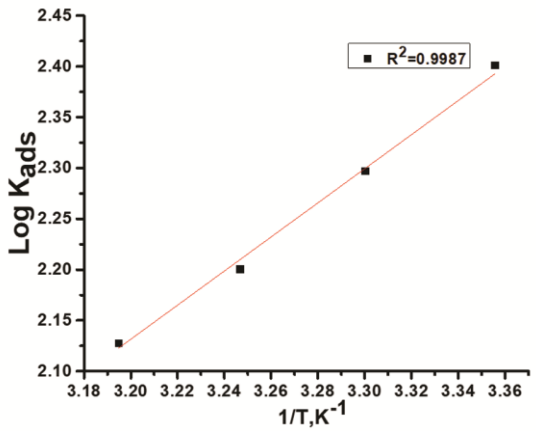

Fig. 5 —Log K_{ads} versus 1000/T for the dissolution of the LCS in presence of MPE

PP measurements

The most common corrosion events are electrochemical in nature and consist of reactions on the surface of corroding metal. Previously, electrochemical approaches could be used to assess corrosion rates and describe corrosion processes. The inclusion of the extract during the polarization process is a criterion for classifying the kind of extract action, such as anodic, cathodic, or mixed. At 25°C, the Tafel polarization curve of LCS in polluted NaCl in existing and absence altered doses of MPE is shown in Fig. 6. The anodic and cathodic current densities of LCS in the presence of MPE were substantially lower than those of the blank. This decline becomes more pronounced as the MPE dose raises. Furthermore, when MPE is added to a 1 M HCl solution, a slight shift in the corrosion potential toward greater positive potentials is seen. The cathodic component shows the emergence of parallel Tafel lines, showing that activation controls hydrogen development. As a result, hydrogen discharge is predominantly accomplished at the LCS surface via a charge transfer mechanism[32]**.** As a result, the inhibition process might be induced by a simple blocking surface effect, such as a decrease in reaction area on the corroding surface0[33,34]. At each concentration, the values of PE and Θ were determined using Eq. 8[35,36].

$$\text{“}\%\ PE = \Theta \times 100 = (1 - i_{corr}/i_{corr(inh)}) \times 100\text{”} \quad \ldots(8)$$

where i_{corr} and $i_{corr(inh)}$ are the corrosion current densities of uninhibited and inhibited solutions, respectively. Table 5 shows that when the extract concentration increases, the i_{corr} values drop. The increase in extract concentration causes a considerable shift in ß$_a$ and ß$_c$, indicating a mixed type of

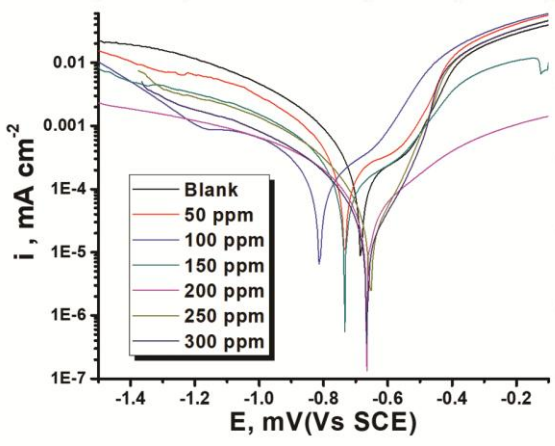

Fig. 6 — PP curves for the corrosion of LCS in NaCl/Na_2S with and without altered concentrations of MPE at 25°C

Table 5 — The impact of the concentration of MPE on the electrochemical parameters calculated by using the PP technique for dissolution of LCS in NaCl/Na_2S at 25°C

Conc. ppm	$-E_{corr}$, mV vs. SCE	i_{corr}, µA cm^{-2}	$-\beta_c$, mV dec^{-1}	β_a, mV dec^{-1}	C.R mmy^{-1}	θ	%PE
Blank	1040±0.4711	264± 0.3154	242± 0.3165	340±0.4511	120	------	-----
50	733± 0.4934	120± 0.4776	11280±0.4354	381±0.5054	58.18	0.545	54.5
100	812± 0.5561	100± 0.4541	270± 0.4722	350±0.2733	49.54	0.621	62.1
150	733± 0.4341	90± 0.2554	281± 0.2622	325±0.3244	42.27	0.659	65.9
200	665± 0.2898	61± 0.5132	294± 0.3376	330±0.5176	30.45	0.769	76.9
250	664± 0.4022	35± 0.6223	245± 0.2534	372±0.4376	17.72	0.867	86.7
300	665± 0.4911	30± 0.3087	239± 0.3687	360±0.3121	15.0	0.886	88.6

inhibitor[37]. The protective efficacy of the extract improved as the concentration of the extract increased. MPE is a mixed-type inhibitor with cathodic action as its main feature. Following the addition of the extract, the polarization curves altered toward a lower negative potential and lower current density values, as shown in Fig. 6, indicating that MPE's protection mode is simple surface blockage by adsorption. The extract species are adsorbed on the metal surface by the donor atoms of oxygen and the electron clouds of the benzene rings, increasing the (θ) as the extract concentration increased. The bulky group of the extract also prevents ions from diffusing to or from the electrode surface[38]. As a result, the anodic dissolution current density of LCS is reduced.

EIS measurements

Impedance measurements are frequently used to gain a better understanding of the process at LCS contact. EIS was carried out in a blank and inhibited solution containing varying concentrations of MPE under potentiostatic conditions at 25°C.Impedance tests reveal how the extract can be produced into a thin layer film on the metal surface. Figure 7 shows the corrosion behavior of LCS with and without MPE in 3.5 percent NaCl and 16 ppm Na_2S. As indicated by Tsuru *et. al*[39]**,** the charge-transfer resistance (R_{ct}) values are determined from the difference in impedance at lower and higher frequencies. The following equation yields the double-layer capacitance (C_{dl}) and the frequency at which the imaginary component of the impedance is maximal ($-Z_{max}$):

$$C_{dl} = \frac{1}{2\pi f_{max} R_t} \quad \ldots(9)$$

Where f_{max} is the maximum frequency at which the imaginary component of the impedance (Z_{im}) is at itsmaximum at $R_t$is the diameter of the loop". The PE_{ct} obtained from the charge transfer resistance is

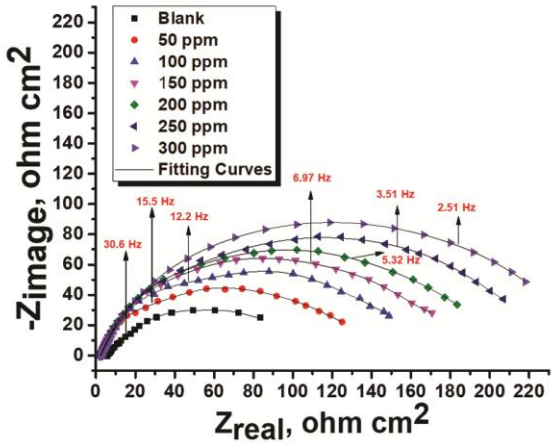

Fig. 7 — Nyquist plots recorded for the LCS in NaCl/Na_2S with and without altered concentrations of MPE at 25°C

calculated by:

s

$$PE_{ct}\% = 100 \times (1 - R_t/R_{t/inh}) \quad \ldots(10)$$

R_t and $R_{t/inh}$ are the charge-transfer resistance values without and with extract, respectively. The semicircle indicates that the corrosion process was primarily controlled by charge transfer[40]. "The general form of the curves is extremely similar for all samples, showing that the addition of the extract had essentially little effect on the corrosion mechanism[41]". The diameter of the Nyquist plots grew as the extract concentration rose. These findings suggested that increasing extract concentrations improves PE. Table 6 shows that raising the extract concentration improve the charge transfer resistance (R_{ct}) while decreasing the double layer capacitance (C_{dl}). The steady replacement of water molecules by extract molecules adsorbing on the metal surface to produce an adherent layer on the metal surface could explain the increase in R_{ct} values and, as a result, protection efficiency. Because of roughness and potential oxide surface imperfections, the n value appears to be connected to the nonuniform distribution of current.

Table 6 — Electrochemical kinetic parameters obtained by EIS technique for the corrosion of LCS using MPEas extract in NaCl/Na_2S at 25°C"

Conc., ppm	$R_{s,}$ Ω cm^2	$C_{dl,}$ µFcm^{-2}	n	$R_{ct,}$ Ω cm^2	θ	%PE
Blank	5.561±0.5111	163.74±0.4343	0.867	31.72	----	----
50	4.171± 0.5554	86.70± 0.2976	0.883	65.34	0.477	47.7
100	4.155± 0.3776	71.62± 0.5232	0.842	84.83	0.575	57.5
150	4.845± 0.4676	64.83± 0.4911	0.897	88.63	0.622	62.2
200	3.359± 0.3798	48.56± 0.4145	0.878	115.46	0.716	71.6
250	4.942± 0.3823	32.03± 0.5567	0.888	130.42	0.823	82.3
300	3.642± 0.2221	25.16± 0.3232	0.878	143.22	0.859	85.9

Table 7 — Electrochemical kinetic parameters obtained by the EFM technique for LCS in 3.5% NaCl+16 ppm Na_2S alone and with different concentrations of MPE at25°C

Conc., ppm	$i_{corr.,}$ µA cm^{-2}	β_a, mV dec^{-1}	$-\beta_c$, mV dec^{-1}	CF-2	CF-3	C.R, mmy^{-1}	Θ	%PE
Blank	678.2±0.3721	135±0.4043	185±0.3534	1.933	2.891	309.9	---	---
50	334.0±0.5433	156±0.3755	201±0.4911	1.881	2.935	152.6	0.508	50.8
100	284.0±0.4954	148±0.4013	196±0.3422	1.980	2.999	129.8	0.581	58.1
150	246.4±0.4332	155±0.4928	207±0.2265	1.890	2.883	112.6	0.637	63.7
200	184.3±0.4054	142±0.4616	211±0.2076	1.923	2.974	84.2	0.728	72.8
250	106.3±0.4911	151±0.3714	194±0.4076	1.875	2.999	48.5	0.843	84.3
300	88.6±0.4311	154±0.3484	212±0.3182	1.969	2.864	40.4	0.869	86.9

CPE indicates a perfect capacitor when n = 1. Because genuine capacitive behavior is rare, CPE is commonly employed for data fitting instead of a perfect capacitor. The current investigation demonstrates that n < 1 in both uninhibited and inhibited media, demonstrating surface heterogeneity despite MPE adsorption on the LCS surface's most active adsorption sites. According to the literature, the modest drop in n is a sign of surface in homogeneity caused by inhibitor adsorption[42]. In our situation, the reverse tendency is seen, indicating an increase in homogeneity when MPEO is adsorbed. The results show that the corrosion efficiency values obtained using the impedance approach and polarization measurements are in good agreement. The corrosion rate is determined by the chemical composition of the electrolyte rather than the technology used[43]. The EIS data were reproduced using equivalent electric circuits, as illustrated in Fig. 8, with R_S denoting solution or electrolyte resistance, C_{dl} denoting double layer capacitance, and R_{ct} denoting charge transfer resistance. The chi square value ($\chi 2$)[44] is used to assess the quality of fitting to the analogous circuit. Table 6 shows the appropriate values (0.0281–0.0951), which demonstrate the high-quality fitting with the suggested circuit.

EFM measurements

With the EFM technique, a potential perturbation by two sine waves of different frequencies is applied

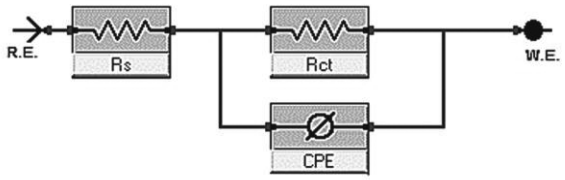

Fig. 8 — Electrical equivalent circuit used to fit impedance data

to a corroding system. As a corrosion process is nonlinear in nature, responses are generated at more frequencies than the frequencies of the applied signal. The AC current response due to this perturbation consists of current components (peaks) of different frequencies. Analysis of these current responses can result in the corrosion rate and Tafel parameters[45]. Fig. 9 shows intermodulation spectra derived from EFM measurements as examples of LCS in 3.5 percent NaCl and 16 ppm Na_2S with and without 300 ppm MPE at 25°C. (i_{corr}, ß$_c$, ß$_a$, CF-2, CF-3, and percent PE) are all corrosion kinetic characteristics of MPE with varied doses in polluted NaCl at25°C in Table 7. As the extract concentration rises, the i_{corr} falls and the protection efficiency rises. The causation factors in Table 7 are quite close to the theoretical values, which should ensure the validity of the Tafel slope and corrosion current densities, according to EFM theory. The %IE obtained from the WL, PP, EIS, and EFM approaches were found to be in consistent with each other.

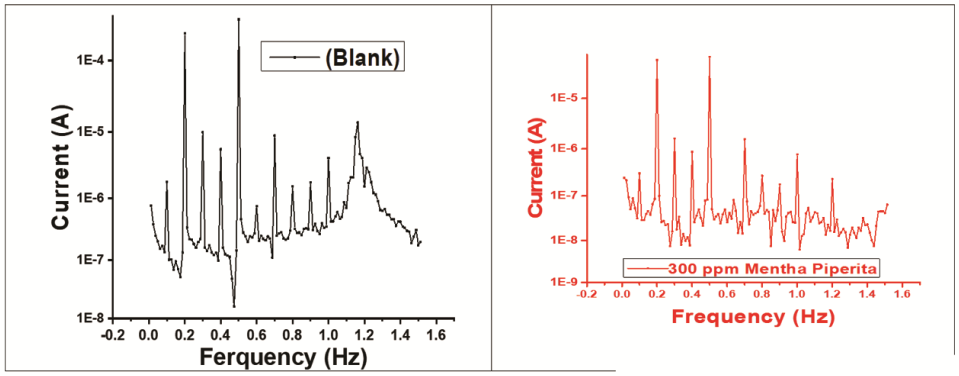

Fig. 9 — Intermodulation spectrum for LCS in 3.5% NaCl+16 ppm Na_2S solution in the absence and presence of different concentrations of MPE at 25ºC

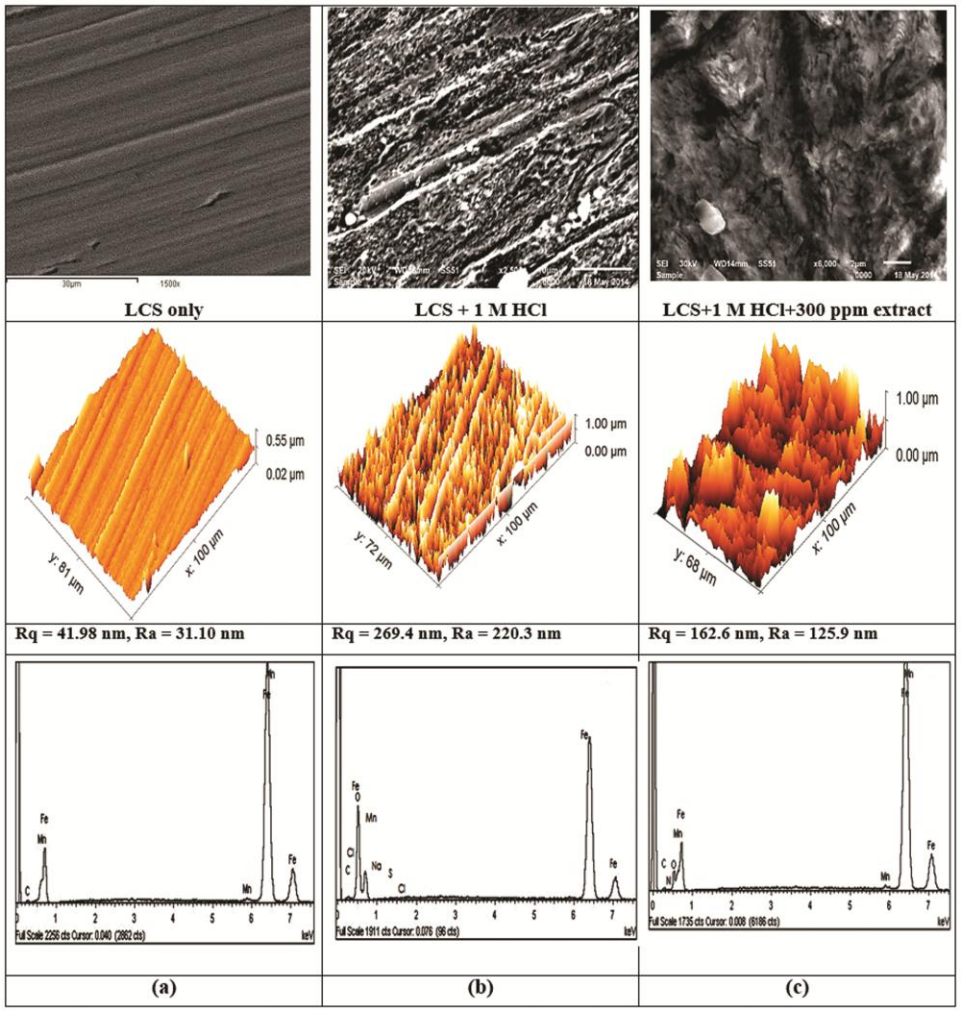

Fig. 10 — SEM micrographs and EDX spectra of the LCS surface recovered from (a) Pure; (b) in corrosive solution and (c) in corrosive solution + 300 ppm extract

Surface characterization

EDX spectra, the corresponding SEM micrographs and AFM of the LCS surface only after dipping in the corrosive media with and without the extract for approximately 5 days are shown in Fig. 10(a-c). The image of LCS surface is presented in Fig. 10a. An image of the LCS surface after dipping in corrosive media for approximately 5 days is presented in Fig.

10(b) showing distortion due to the porous oxide film layer. The result of adding the extract to the metal surface is shown in Fig 10(c), where there is no surface damage, and the surface is smooth. The metal sample is linked to the distinctive peaks. The metal surface has peaks of Fe, Mn, Cl, Na,S, and oxygen atoms after immersion in the corrosive fluids for approximately 5 days, as shown in Fig. 10(b), which is connected to the oxide film generated on the metal surface. Fig. 10(c) shows the SEM peaks of the effect of the addition of the extract on the metal surface. In Fig. 10(c), the peaks of Fe decrease, and the peaks of oxygen increase, which indicates great coverage of the extract on the metal surface, leading to a decrease in the peaks of the Fe atoms, and the extract passivates the metal surface from the corrosive media. Therefore, MPE is a good extract for LCS at a 300-ppm concentration.

Biological effect of MPE on *Escherichia Coli*

In the absence and presence of MPE, bacterial agriculture of *Escherichia coli* is carried out. There was no influence on the activity of Escherichia coli, as shown in Table 8. The MPE, which has an oxygen donor atom, is hypothesized to connect to the proteins and lipids of bacterial tissues, assisting in the respiration process. As a result, this extract has no toxicity on bacterial activity and may be safely used in sanitation facilities without causing any problems in the treatment process.

Mechanism of corrosion protection

Some MPE molecules can be protonated in the corrosive medium (acquire + ve charge), and the LCS has a positively charged surface, so there is repulsion between it and the protonated molecules. The Cl^- ions areadsorbed on the LCS surface and turn its surface negative, after which the protonated molecules are adsorbed on the –ve LCS surface (Scheme 1). Diterpenes, steroids, tannins, flavonoids, carbohydrates, alkaloids, phenols, coumarin, and saponins are the primary chemical elements of the phytochemical MPE extract[22]. Most of these phytochemicals are organic molecules with polar functional groups of oxygen (O) and nitrogen (N). A structure such as this promotes the creation of a complex with dissolved iron ions. The production of insoluble complexes is indicated by the result. These complexes are adsorbed onto the LCS by weak pressures, forming a protective layer against the corrosive environment and therefore slowing the dissolving process.

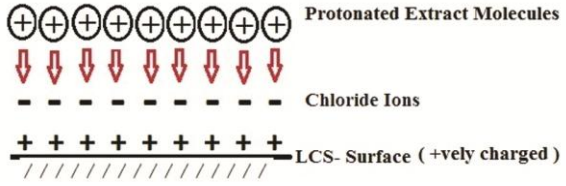

Scheme 1 — Corrosion inhibition mechanism

Conclusion

The following data can be drawn based on the obtained data:

In sulfide polluted saltwater, MPE works as a corrosion inhibitor for LCS, with an efficiency of 87.43 percent at a 300 ppm concentration. MPE adsorption on metal surfaces follows the Temkin adsorption isotherm, indicating that it is an effective eco-friendly and low-cost extract. As the temperature rises, the effectiveness of the protection system decreases. Strong and spontaneous adsorption of MPE on the metal surface is indicated by the negative free energy ($-\Delta G^o_{ads}$) of adsorption. The Tafel constant values ($ß_a$ and $ß_c$) indicate that the extract is a mixed type with a cathodic component. Adsorbed species formed insoluble complex compounds when they came into contact with dissolved iron ions. The protection efficiencies reported using various electrochemical methods is consistent. Because this extract has no influence on *Escherichia coli* biological activity, it can be used safely in sanitation plants.

References

1 Eddy N, *Int J Phys Sci*, 4 (2009) 165.
2 Eddy N, Odoemelam S A & Akpanudoh N W, *Res J Pure Appl Sci*, 4 (2008) 1963.
3 Sultan A A, Ateeq A A, Khaled N I, Taher M K & Khalaf M N, *J Mater Environ Sci*, 5 (2014) 498.
4 Selles C, Benali O, Tabti B, Larabi L & Harek Y, *J Mater Environ Sci*, 3 (2012) 206.
5 Khadraoui A, Khelifa A, Boutoumi H, Hamitouche H, Mehdaoui R & Hammouti B & Al-Deyab S S, *Int J Electrochem Sci*, 9 (2014) 3334.
6 Verma C B, Quraishi M A & Ebenso E E, *Int J Electrochem Sci*, 9 (2014) 5507.
7 Fouda A S, El-Hossiany A & Ramadan H, *Zast Mater*, 58 (2017) 541.
8 Fouda A S, Mohamed O A & Elabbasy H M, *J Bio Tribo Corros*, 7 (2021) 1.
9 Kamel M M, Fouda A A S, Rashwan S M & Abdelkader O, *Green Chem Lett Rev*, 14 (2021) 598.
10 Fouda A S, Al-Hazmi N E, El-Zehry H H & El-Hossainy A, *J Appl Chem*, 9 (2020) 362.
11 Majidi L, Faska Z, Znini M, Kharchouf S, Bouyanzer A & Hammouti B, *J Mater Environ Sci*, 1 (2010) 219.
12 Znini M, Cristofari G, Majidi L, Ansari A, Bouyanzer A & Paolini J, Costa J & Hammouti B, *Int J Electrochem Sci*, 7 (2012) 3959.

13 Chraibi M, Benbrahim K F, Elmsellem H, Farah A, Abdel-Rahman I, El Mahi B, Filali Baba Y, Kandri Rodi Y & Hlimil F, *J Mater Environ Sci*, 8 (2017) 972.

14 Belkhaouda M, Bammou L, Salghi R, Benali O, Zarrouk A & Ebenso E E, Hammouti B, *J Mater Environ Sci*, 4 (2013) 1042.

15 Fouda A S, Badr S E, Ahmed A M & El-Hossiany A, *Int J Corros Scale Inhib*, 10 (2021) 1011.

16 Afia L, Salghi R, Bazzi E, Bazzi L, Errami M & Jbara O, Al-Deyab S S & Hammouti B, *Int J Electrochem Sci*, 6 (2011) 5918.

17 Salhi A, Bouyanzer A, Hamdani I, Chetouani A, Hammouti B & Znini M, Majidi L, Costa J & El Azzouzi M, *Der Pharma Chem*, 7 (2015) 138.

18 Fouda A S, El-Gharkawy E S, Ramadan H & El-Hossiany A, *Biointerface Res Appl Chem*, 11 (2021) 9786.

19 Halambek J, Berković K & Vorkapić-Furač J, *Corros Sci*, 52 (2010) 3978.

20 Zerga B, Sfaira M, Rais Z, Touhami M E, Taleb M & Hammouti B, *Matériaux Tech*, 97 (2009) 297.

21 Hussin M H, Rahim A A, Ibrahim M N M & Brosse N, *Measurement*, 78 (2016) 90.

22 Sachinkumar P R, Patil R S & Godghate A G, *Int J Pharm Pharm Sci*, 8 (2016) 352.

23 Sroka Z, Fecka I & Cisowski W, *Zeitschrift für Naturforsch C*, 60 (2005) 826.

24 Fouda A S, El-Wakeel A M, Shalabi K & El-Hossiany A, *Elixir Corros Day*, 83 (2015) 33086.

25 Singh A, Singh V K & Quraishi M A, *Rasayan J Chem*, 3 (2010) 811.

26 Bentiss F, Traisnel M, Chaibi N, Mernari B, Vezin H & Lagrenée M, *Corros Sci*, 44 (2002) 2271.

27 Popova E, Sokolova S, Raicheva S & Christov M, *Solut Corros Sci*, 45 (2003) 33.

28 Al-Sarawy A A, Fouda A S & El-Dein W A S, *Desalination*, 229 (2008) 279.

29 Fouda A S, Shalabi K & E-Hossiany A, *J Bio Tribo Corros*, 2 (2016) 1.

30 El-Sherbini E E F, *Mater Chem Phys*, 60 (1999) 286.

31 Fouda A S, Azeem M A, Mohamed S & El-Desouky A, *Int J Electrochem Sci*, 14 (2019) 3932.

32 Fouda A S, Abd El-Maksoud S A, Belal A A M, El-Hossiany A & Ibrahium A, *Int J Electrochem Sci*, 13 (2018) 9826.

33 Fouda A S, Rashwan S, El-Hossiany A & El-Morsy F E, *J Chem Biol Phys Sci*, 9 (2019) 1.

34 Fouda A S, Abdel-Latif E, Helal H M & El-Hossiany A, *Russ J Electrochem*, 57 (2021) 159.

35 Fouda A S, Ibrahim H, Rashwaan S, El-Hossiany A & Ahmed R M, *Int J Electrochem Sci*, 13 (2018) 6327.

36 Motawea M M, El-Hossiany A & Fouda A S, *Int J Electrochem Sci*, 14 (2019) 1372.

37 Fouda A S, Eissa M & El-Hossiany A, *Int J Electrochem Sci*, 13 (2018) 11096.

38 Fouda A S, El-Dossoki F I, El-Hossiany A & Sello E A, *Surf Eng Appl Electrochem*, 56 (2020) 491.

39 Elgyar O A, Ouf A M, El-Hossiany A & Fouda A E A S, *Biointerface Res Appl Chem*, 11 (2021) 14344.

40 Fouda A S, Ahmed R E & El-Hossiany A, *Prot Met Phys Chem Surfaces*, 57 (2021) 398.

41 Khaled M A, Ismail M A & Fouda A E S, *RSC Adv*, 11 (2021) 25314.

42 El Hamdani N, Fdil R, Tourabi M, Jama C & Bentiss F, *Appl Surf Sci*, 357 (2015) 1294.

43 Raja P B, Qureshi A K, Rahim A A, Osman H & Awang K, *Corros Sci*, 69 (2013) 292.

44 Fouda A S, Abd El-Ghaffar M A, Sherif M H, El-Habab A T & El-Hossiany A, *Prot Met Phys Chem Surfaces*, 56 (2020) 189.

45 Rauf A & Mahdi E, *Int J Electrochem Sci*, 7 (2012) 4673.